Fabrication of Bi_2MoO_6 Photocatalytic Fibers via Wet Spinning and Enhanced Photocatalytic Activity

Jun Sun[1,3], Yan Zhang[1,*], Xiaobing Tian[1,2,3], Meijun Yang[1], Xiaolong Yang[1] and Jianqiang Yu[1,*]

[1] Institute of Green Chemistry and Industrial Catalysis, School of Chemistry and Chemical Engineering, Qingdao University, Qingdao 266071, China;
[2] Resources and Environmental Engineering, Wuhan University of Technology, Wuhan 430070, Hubei, China;
[3] Qingdao Rongchuang Institute of Novel Materials, Qingdao International Academician Park, Qingdao 266000, China.

Abstract. In this paper, Bi_2MoO_6 photocatalytic fibers were fabricated by wet spinning method and the photocatalytic activity was found to be enhanced significantly. The Bi_2MoO_6 powders were prepared by hydrothermal process at different pH (0.4, 6, 8, 10), which is recorded as BMO-0.4, BMO-6, BMO-8, BMO-10. The powders were then mixed with sodium alginate colloid, and fabricated into photocatalytic fibers by wet spinning. The samples were recorded as FB-0.4, FB-6, FB-8, FB-10, respectively. The crystal phase, morphology and photophysical properties of the fiber samples were characterized by X-ray powder diffraction (XRD), scanning electron microscopy (SEM), and laser particle size analysis (LPSA). In order to investigate the photocatalytic performance of the synthesized photocatalysts, RhB and formaldehyde were used as simulated water pollutant and air pollutant, respectively. It showed that the efficiency of the degradation of RhB over BMO-10 was 75%, while that enhanced to 85% over FB-10. It should be noted that the content of photocatalyst in the fiber FB-10 was only 1%. The degradation efficiency of formaldehyde in FB-10 sample reaches 92%.

1. Introduction

With the development of the economy and the progress of society, environmental pollution and energy shortage are two major problems that human beings urgently need to solve. Since Fujishima and Honda reported the use of TiO_2 as a photoanode for UV photolysis of water [1], Bard reported that UV-irradiation of TiO_2 can transform CN^- to OCN^- [2], and more and more scholars have set their sights on it. Among the semiconductor materials for photocatalysis, visible-light semiconductor materials have become attractive photocatalysts due to their excellent light-absorption properties, adjustable band gap and low cost [3]. Bismuth molybdate is one of the representative materials. A

large number of scholars have studied the doping of bismuth molybdate to form heterojunctions [4], but the application research on bismuth molybdate-based materials has not been developed.

Regarding the investigation of photocatalytic fibers, the most widely studied is TiO_2 photocatalytic fiber, and the photocatalytic performance of the fiber is studied by attaching TiO_2 to the fiber. For example, Yuan [5] research group connected the TiO_2 and activated carbon fiber with the calcined epoxy resin residue, and explored the relationship between the pore size of the fiber and its photocatalytic performance. Zhong [6] research group used hollow fiber (HOF) to combine with TiO_2 matrix composites to improve the photocatalytic activity. Cai [7] studied the preparation of TiO_2 fibers with cotton fibers as template, and then synthesized Ag_3PO_4/TiO_2 fibers by in-situ growth method on Ag_3PO_4 particles. However, TiO_2 can only be excited by ultraviolet light to generate electrons and holes, and photogenerated electrons and holes are easily recombined, resulting in low utilization of light energy. These problems limit its wide application.

The currently prepared photocatalytic fiber method mainly combines the photocatalyst with the fiber by a suitable binder, or directly adds the photocatalyst to the spinning solution and directly spun it by electrospinning or wet spinning. The alginic acid used in this paper is a linear polymer polyelectrolyte [8] extracted from the marine organism brown algae, which has a wide range of sources, environmental protection, biocompatibility, high hygroscopicity, flame retardancy, gel blocking, high oxygen permeability, high ion adsorption, antibacterial, and many other excellent properties. It has a wide range of applications in the fields of biology, food, textile, medical and health. The photocatalyst is used to control different pH values to prepare different structures of bismuth molybdate material [9], and the synthetic material is stirred and mixed with sodium alginate to form a colloid, and the photocatalytic fiber is directly spun by wet spinning. The degradation properties of different fibers to RhB and formaldehyde were investigated under visible light.

2. Experimental Method

2.1. Material preparation

$(NH_4)_6Mo_7O_{24}·4H_2O$ (0.72 mmol) was sonicated in 20 mL of H_2O, and $Bi(NO_3)_3·5H_2O$ (10 mmol) was completely dissolved in 20 mL of HNO_3 solution (2.0 mol·L^{-1}) and stirred for 30 min. The cerium nitrate solution was added dropwise to the ammonium molybdate solution under magnetic stirring. The pH of the mixture was adjusted to 0.4, 6, 8, and 10 using ammonia water. Stir for 30 minutes. The mixture was transferred to a reaction kettle and heated at 150 °C for 24 hours. The product was taken out, washed with deionized water to neutrality, and then dried at 60 °C for 8 hours to obtain Bi_2MoO_6 synthesized under different pH conditions. Recorded as BMO-0.4, BMO-6, BMO-8, and BMO-10.

20g $(C_6H_7O_6Na)_n$ was slowly poured into 450g of H_2O, stirred evenly to form a colloid. 5g of the obtained Bi_2MoO_6 was added to the colloid, stirred for 24 hours, placed in a spinning machine for 2 h, and $CaCl_2$ was used as a coagulating liquid. Compared with 1:1.2, spinning for one hour, photocatalytic fibers were obtained. The photocatalytic fibers prepared from Bi_2MoO_6 prepared at different pH values of 0.4, 6.0, 8.0, and 10.0 were recorded as FB-0.4, FB-6, FB-, 8, FB-10.

2.2. Sample Characterization

X-ray diffraction (XRD) spectra of the samples were measured on a Bruker D8-advance X-ray diffractometer. The experiment used Cu Ka target n = 0.15478 nm), and the scanning range was 5 °to

80 ℃. Scanning electron microscopy (SEM) characterization was performed on a JSM-6700F field emission scanning electron microscope. Laser particle size analysis (LPSA) was performed on a Winner 2005 laser particle size analyzer.

The degradation of RhB was carried out by irradiating RhB under a 500 W xenon lamp (cut filter $\lambda \geq 420$ nm), and the photocatalytic suspension was subjected to photocatalytic activity. In the degradation experiment, 40 mg of Bi_2MoO_6 photocatalyst was dispersed in 40 mL of RhB dye solution (4.0 mg L^{-1}) and stirred in the dark for 60 minutes to achieve desorption-adsorption equilibrium. 500 mg of the photocatalytic fiber was dispersed in 200 mL of RhB dye solution (1.0 mg L^{-1}) and stirred in the dark for 60 minutes to reach a desorption-adsorption equilibrium, after which the above suspension was irradiated with a light source at a distance of 10 cm. During the photocatalytic reaction, 4 mL of the liquid was taken out from the reactor at intervals of 30 minutes, and then the photocatalyst was separated by centrifugation. The ultraviolet absorption peak of the catalyst-free RhB solution was measured at 554 nm using a spectrophotometer.

Formaldehyde degradation was carried out in a self-made $1m^3$ reaction chamber. The sample fibers were arranged on the same length of 50×50cm transparent glass, placed in the center of the tank, and the continuous formaldehyde tester was connected to the tank with a leather tube. The internal formaldehyde concentration, using a specific method, so that the concentration of formaldehyde gas in the cabin is $1mg/m^3$, recorded as c_0, open 30w fluorescent lamp for irradiation, record the data once every 0.5h, record as c, for 8h, then the degradation efficiency is $(1 - c/c_0)$.

3. Results and Discussion

3.1. Phase Structure Analysis of Bi_2MoO_6

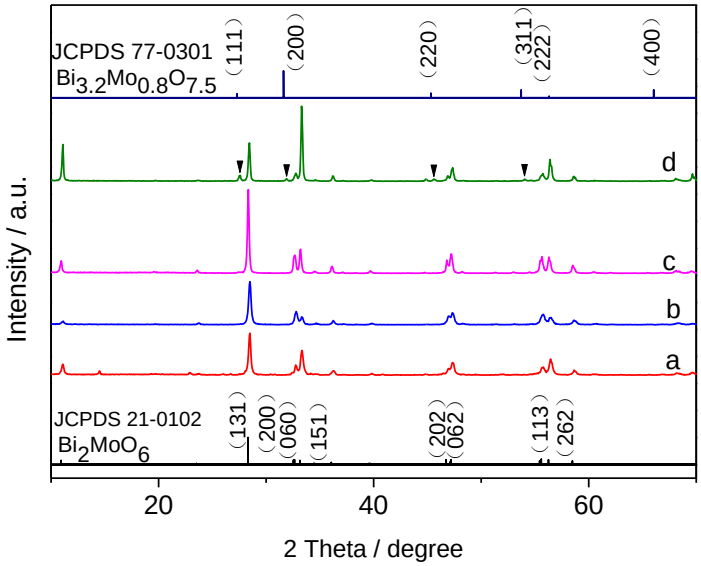

Figure1. XRD Spectrum of Bi_2MoO_6 Prepared under Different pH Conditions
(a) pH=0.4; (b) pH=6; (c) ph=8; (d)=10

Figure 1 is a XRD pattern of the product prepared at different pH values. It can be seen from the figure that the diffraction peak intensity of all the samples is large and the peak is sharp, which indicates that the sample prepared by hydrothermal method has good crystallinity. (020), (131), (200), (002), (060), (151), (202), (113), (262) crystal planes appeared in the four groups of samples, indicating that there are γ-Bi2MoO6 in the substance. When the pH value is 0.4, it can be seen from the XRD spectrum that the product is a composite phase of Bi_2MoO_6 and Bi_2O_3. As the pH value increases, the product becomes pure phase Bi_2MoO_6, and the crystallinity of pH 8 is better than the crystallinity of pH 6, and at pH 8, the (111), (200), (220) , (311), (222), (400) crystal plane, indicating that $Bi_{3.2}Mo_{0.8}O_{7.5}$ gradually appeared in the product. When the pH reached 10, it was obvious that orthogonal γ-Bi_2MoO_6 and $Bi_{3.2}Mo_{0.8}O_{7.5}$ existed in the product, it is expected that a $Bi_{3.2}Mo_{0.8}O_{7.5}$ quantum dot modified Bi_2MoO_6 has a heterojunction structure with special properties such as quantum size effect, which is consistent with previous reports.

Figure 2 is a SEM photograph of Bi_2MoO_6 prepared under different pH conditions. It can be seen from the SEM photograph that the four groups of samples are mainly in the form of a sheet, the size of the first three particles are below 1 μm, and the size of the fourth particle is about 3 μm. When the pH reaches 8, spherical particles appear, $Bi_{3.2}Mo_{0.8}O_{7.5}$ appears, which is consistent with the XRD characterization. $Bi_{3.2}Mo_{0.8}O_{7.5}$ forms quantum dots on the surface of γ- Bi_2MoO_6, which is heterogeneous. Junction structure, such a structure helps to improve its photocatalytic efficiency. The synthesized particles are all around 1μm.

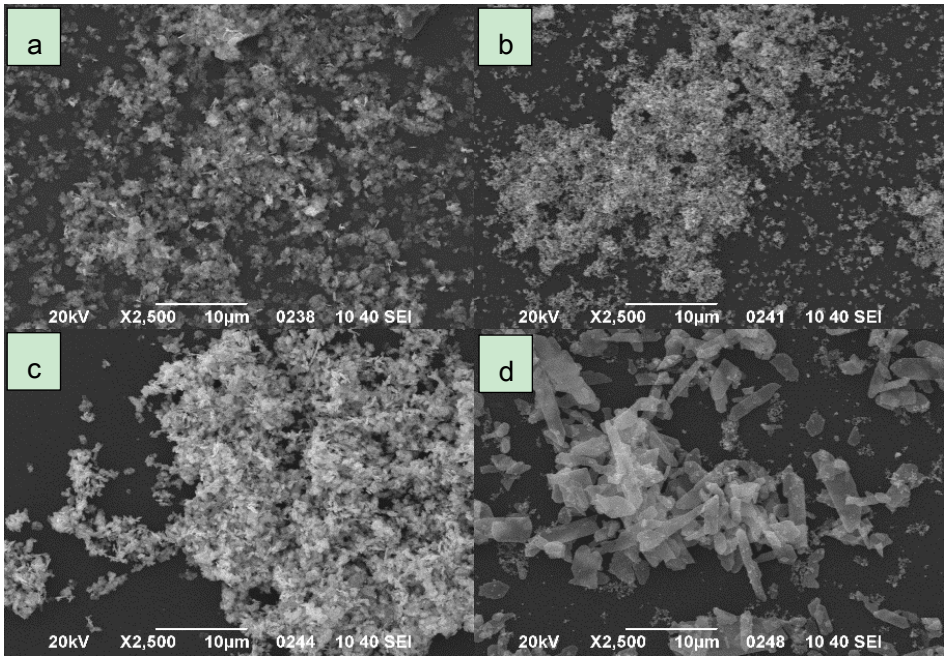

Figure 2. SEM Photograph of Bi_2MoO_6 Prepared under Different pH Conditions (a) BMO-0.4, (b) BMO-6, (c) BMO-8, (d) BMO-10

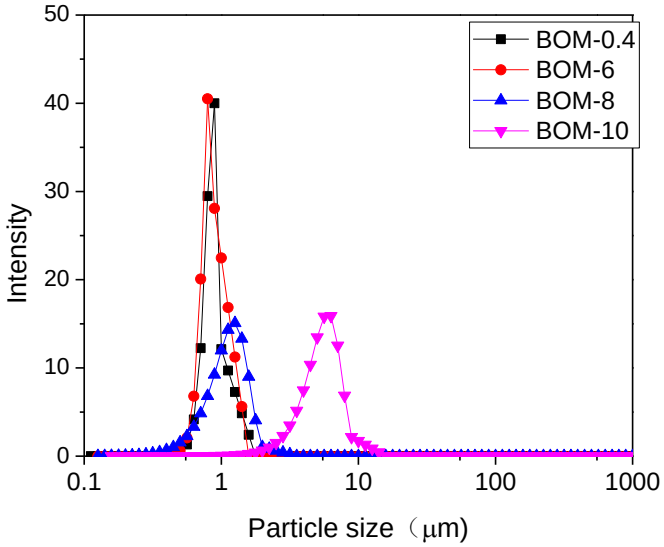

Figure 3. Laser Particle Size Analysis of Samples Prepared at Different pH Values

Figure 3 is a laser particle size spectrum obtained by the test, where in the sample particle size obtained by pH 0.4 is between 0.664-0.907μm, the sample size of pH 6 is between 0.563-0.765μm, and the sample size of pH 8 is The sample size of 0.559-1.320μm and pH 10 was between 2.238 and 4.979μm, which is consistent with the particle size data obtained by SEM. Such particle size ensures the progress of the wet spinning experiment.

3.2. Phase Structure Analysis of Fiber Samples

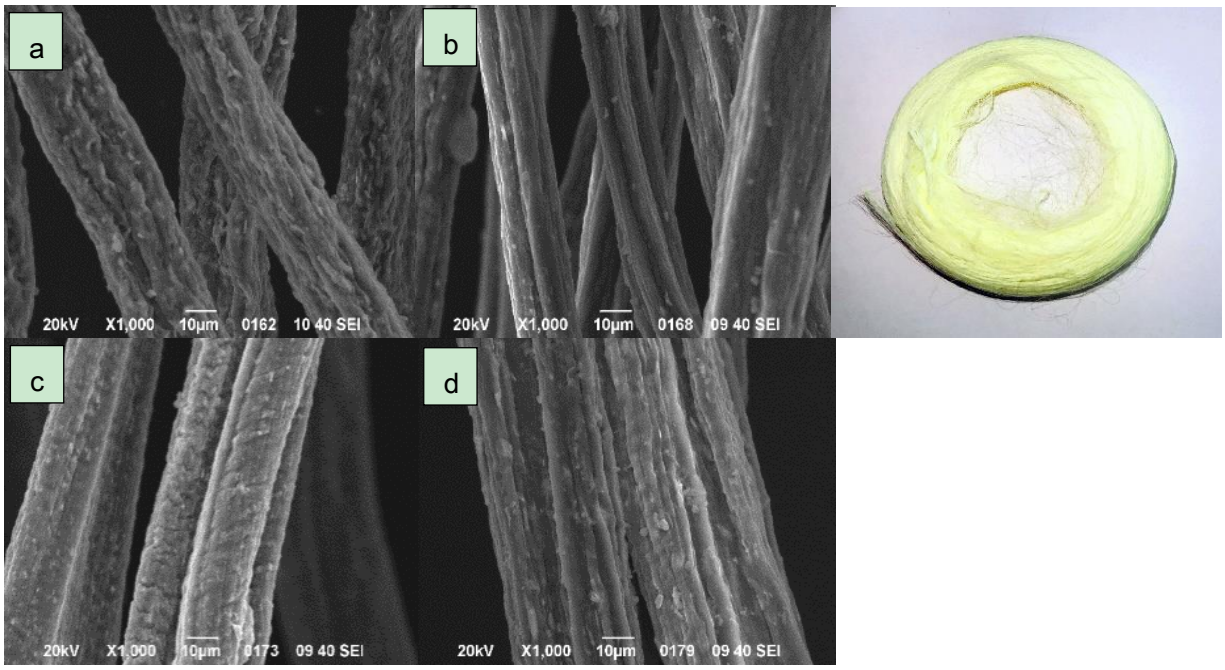

Figure 4. A. SEM Photographs of Fibers Made from Different Samples (a) FB-0.4, (b) FB-6, (c) FB-8, (d) FB-10 B. Apparent Photo of the Fiber Sample

Figure 4 is a SEM photograph of a photocatalytic fiber obtained by a wet spinning method. It can be seen from the picture that the fiber diameter is about 15μm, the aspect ratio is large, the thickness is relatively uniform, the surface is rough, and there are many tiny The particles are distributed on the surface of the fiber, and the distribution is relatively uniform and fine, and no agglomeration occurs. It proves that we successfully woven the photocatalyst into the fiber by the wet spinning method and the morphology is uniform. It is also apparent from the appearance that the fiber sample changes from white to light yellow fiber, and the distribution is fine, the touch is grain-free, and the photocatalyst and the fiber are well connected.

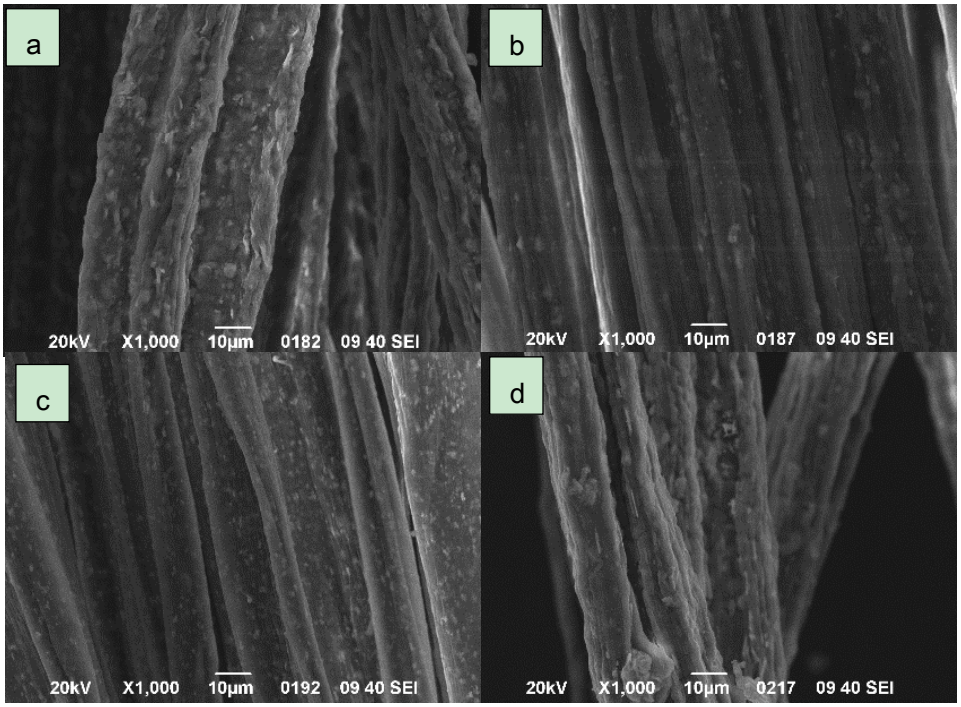

Figure 5. SEM Photograph of Fibers Soaked in Soapy Water for 1 Week

Figure 5 is a SEM picture of the obtained fiber soaked in soapy water for one week. It can be seen from the figure that the surface of the fiber is still attached with many tiny particles, and the distribution is still uniform, which is almost the same as the SEM picture of the fiber before soaking. It can be proved that the photocatalyst in the obtained photocatalytic fiber is relatively strong in connection with the fiber and is not easily broken.

3.3. Photocatalytic Property Investigation

Figure 6 is a graph showing the degradation curves of RhB by powder and photocatalytic fiber under visible light. It can be seen from Figure (a) that the sample prepared by pH 0.4 has a low catalytic performance and can only reach about 10%. The sample prepared at pH 0.6 is pure phase γ- Bi_2MoO_6, and its degradation efficiency can only reach about 25%. With the formation of $Bi_{3.2}Mo_{0.8}O_{7.5}$ and γ-Bi_2MoO_6 heterojunction, the degradation efficiency of the sample is improved. The degradation efficiency of BMO-8 reached 60%, and the degradation efficiency of BMO-10 reached 75%. Figure (b)

shows the degradation RhB spectrum of the photocatalytic fiber produced. The degradation efficiency of FB-0.4 and FB-6 samples is very low, only about 10%, and the degradation efficiency of sample FB-8 can reach 60%. The FB-10 sample can reach about 85%. The degradation trend of the powder sample and the fiber sample is the same, in which the powder degrades 4 mg/L of RhB and the photocatalytic fiber degrades 1 mg/L of RhB. It is worth noting that the photocatalyst content in the fiber sample is only 1%. In this way, the photocatalyst adheres to the surface of the fiber, which greatly improves its photocatalytic performance.

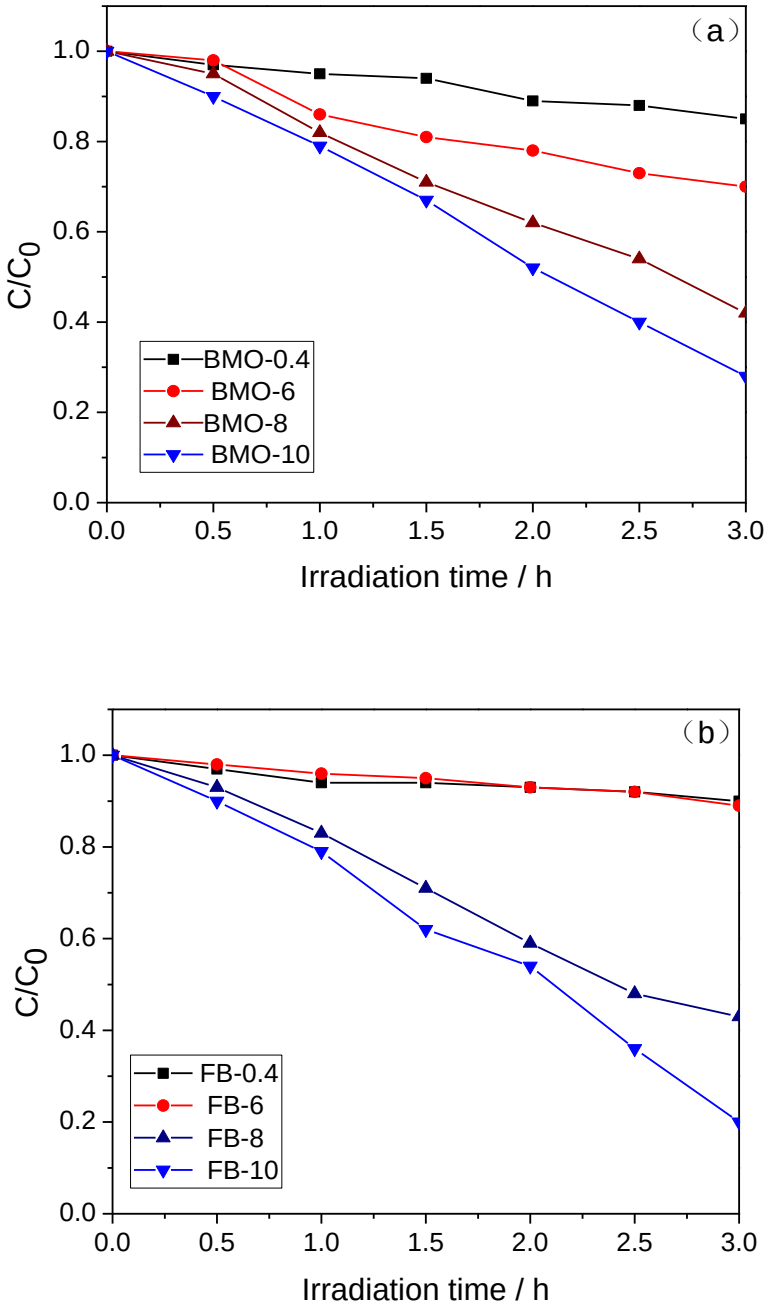

Figure 6. (a) Degradation Curve of RhB in Powder under Visible (b) Degradation of RhB by Photocatalytic Fibers under Visible Light

Figure 7 shows the degradation curve of formaldehyde produced by photocatalytic fiber, which is the same as the degradation of RhB. The degradation efficiency of FB-0.4 and FB-6 to CH2O is only about 15%.with the increase of $Bi_{3.2}Mo_{0.8}O_{7.5}$. The degradation efficiency of the fiber sample prepared by the formation of the heterojunction is greatly improved. The degradation efficiency of the sample prepared at pH 8 is about 70%, and the degradation efficiency of the FB-10 sample is over 92%.

The improvement of photocatalytic performance is due to its uniform distribution on the surface of the fiber, and the surface of the fiber is uneven, which greatly increases the contact area of the material with light and contaminants. The increase in specific surface area makes the degradation efficiency greatly improved.

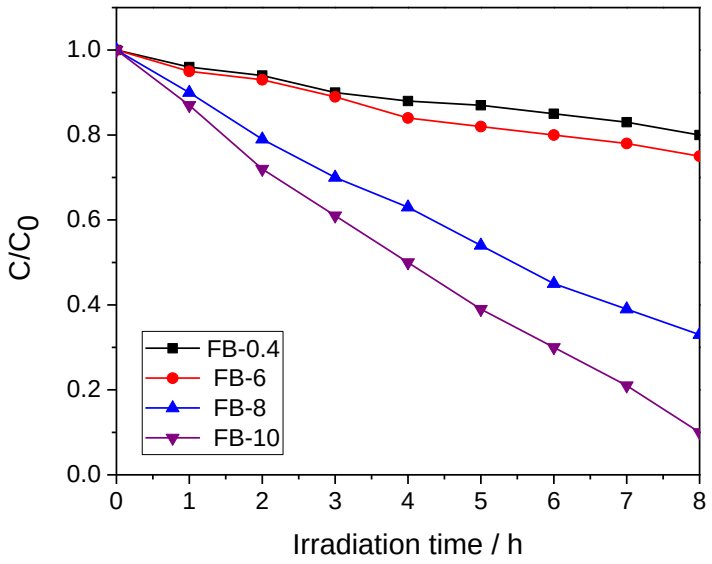

Figure 7. Degradation Curve of Photocatalytic Fiber on CH_2O under Visible Light

4. Conclusion

In this paper, catalyzed thermal and wet spinning methods were used to successfully prepare photocatalytic fibers with high catalytic performance. Among them, γ-Bi_2MoO_6 and $Bi_{3.2}Mo_{0.8}O_{7.5}$ were synthesized under hydrothermal conditions of pH 10,150 ℃. The heterojunction structure sample has high catalytic performance. The degradation efficiency of RhB is about 75% at 3h. The photocatalytic fiber produced by this sample has a degradation efficiency of 85% for 3h, and the degradation efficiency is improved. At the same time, only 1% of the light is contained. The catalyst, such that the degradation efficiency of the photocatalyst is greatly improved compared to the powder. Among them, the degradation of formaldehyde by fiber samples reached more than 92%, and it has high degradation efficiency. In the face of the increasingly serious air pollution and water pollution, the fiber produced in this paper can be used for both water pollution treatment and air pollution treatment. It has a wide application prospect. With the deepening of research, it is believed that it is in the environment. Governance can do a lot.

5. References

[1] Fujishima A, Honda K. Electrochemical photolysis of water at a semiconductor electrode [J]. Nature, 1972, 238 (5358): 37−38.

[2] Frank SN, Bard A J. Heterogeneous photocatalytic oxidation of cyanide ion in aqueous solutions at titanium dioxide powder [J]. J Am Chem Soc, 1977, 99(1): 303−304.

[3] Cao S, Zhou P, Yu J. Recent advances in visible light Bi-based photocatalysts [J]. Chinese Journal of Catalysis, 2014, 35(7): 989-1007.

[4] Hao, Z.; Xu, L. Q.; Wei, B.; Fan, L. L.; Liu, Y.; Zhang, M. Q.;Gao, H. Nanosize α-Bi_2O_3Decorated Bi_2MoO_6 via an Alkali Etching Process for Enhanced Photocatalytic Performance. RSC Adv. 2015, 5, 12346-12353.

[5] Rusheng Yuan, Rongbo Guan, Jingtang Zheng. Effect of the pore size of TiO_2-loaded activated carbon fiber on its photocatalytic activity [J]. Scripta Materialia. 2005, 52: 1329-1334.

[6] Nianbing Zhong, Ming Chen, Yihao Luo, Zhengkun Wang, Xin Xin, Bruce E. Rittmann. A novel photocatalytic optical hollow-fiber with high photocatalytic activity for enhancement of 4 chlorophenol degradation [J]. Chemical Engineering Journal.2018, 355: 731-739.

[7] Li Cai, Qiyi Long, Chao Yin. Synthesis and characterization of high photocatalytic activity and Stable Ag_3PO_4/TiO_2 fibers for photocatalytic degradation of black liquor [J]. Applied Surface Science, 2014, 319: 60-67.

[8] LIU L, JIANG L, XU G K, et al. Potential of alginate fibers incorporated with drug-loaded nanocapsules as drug delivery systems [J]. Journal of Materials Chemistry B, 2014, 2(43): 7596-7604.

[9] Yanhua Peng, Qinghua Liu, Jinqiu Zhang, Yan Zhang, Mengjie Geng, and Jianqiang Yu, Enhanced Visible-Light-Driven Photocatalytic Activity by 0D/2D Phase Heterojunction of Quantum Dots/Nanosheets on Bismuth Molybdates [J]. Phys. Chem. C, 2018, 122: 3738-3747.